Cement and Concrete Research 40 (2010) 924–934

Contents lists available at ScienceDirect

Cement and Concrete Research

journal homepage: http://ees.elsevier.com/CEMCON/default.asp

Effect of moisture conditions and transfers on alkali silica reaction damaged structures

Stéphane Multon [a,*], François Toutlemonde [b]

[a] Université de Toulouse; UPS, INSA; LMDC (Laboratoire Matériaux et Durabilité des Constructions); 135, avenue de Rangueil; F-31 077 Toulouse Cedex 04, France
[b] Université Paris-Est, Laboratoire Central des Ponts et Chaussées (LCPC), 58, bd Lefebvre, 75 732 Paris Cedex 15, France

ARTICLE INFO

Article history:
Received 1 October 2009
Accepted 13 January 2010

Keywords:
Alkali Silica Reaction (C)
Expansions (C)
Modeling (E)
Stress effect (C)
Water effect

ABSTRACT

The aim of this paper is to point out the water driving effect on the alkali silica reaction (ASR) expansion and particularly when modifications of moisture conditions occur. After being submitted to a unidirectional moisture gradient during 14 months, the upper faces of ASR reactive beams were covered by water for 9 months. This late water supply on the upper face rapidly produced large expansions, which mainly occurred along the transverse and the vertical directions resulting in large longitudinal cracks. Companion nonreactive specimens were kept in the same environmental conditions in order to quantify the basic characteristics of moisture-dependent expansive behaviour of the material. The paper focuses on the effects of late water supply or late drying on already ASR-damaged concrete, which is a significant concern for real-life structures. Both structural effects of late water supply on ASR progress in already damaged structures and interpretation of such phenomena are described.

1. Introduction

A large experimental program was carried out at the Laboratoire Central des Ponts et Chaussées (LCPC—Public Works Research Agency), with Electricité de France (EDF—French Power Company) as a partner. The aim was to provide numerous measurements on specimens and beams damaged by alkali silica reaction (ASR) [1–6] in order to validate structural models especially dedicated to ASR-affected structures reassessment [7–14]. The effects of moisture conditions [3,5] and of applied stresses on ASR expansions [6] were studied on a same reactive concrete on specimens and laboratory structures. Thus, it is possible to calibrate models on the behaviour of specimens submitted to various moisture and stress conditions and to validate the calculations in predicting the structural responses as already performed in [14].

The water driving effect on ASR expansions has already been well-described [14–19] and usually taken into account in the modeling. However, another still debated question is the behaviour of reactive materials and ASR gel with respect to late water supply [17,20]. Does ASR gel swell quickly and significantly if large water supply comes into contact with concrete already damaged by ASR? Moreover, when ASR-damaged concrete dries, are the shrinkage strains more or less large than for an undamaged concrete? This may be relevant concerns in the case of the variable moisture conditions of real-life ASR-damaged structures submitted to alternate variations in external relative humidity.

In order to analyze ASR development in such conditions, specimens which were previously kept either in air at 100% RH or sealed under watertight aluminium during two years, were put in water; and specimens kept in water for 2 years also, were exposed to drying air at 30% RH. Their mass variations and deformations were measured. The material response to these new moisture conditions was monitored and is presented in Section 2 of this paper. Moreover, the consequences of such changes in moisture conditions were studied on structures. As described in previous papers, the studied structures were 3 m long, 0.25 m thick and 0.5 m high simply supported beams [1–5]. After 14 months-exposure to a unidirectional moisture gradient (430 days with bottom immersed in water and upper face exposed to a 30% Relative Humidity environment—Figs. 1 and 2), the beams were significantly damaged [3]. In fact, the ASR expansions had reached an asymptotic value in an increasing bottom part of the beams, while drying had progressively stopped the development of ASR between the upper face and the depth of 100 mm [2,3]. The structural analysis of the beams during this period has been presented in [5]. Then, the upper faces of the beams were covered by water and subsequent evolution was monitored for 9 months under the late water supply conditions. The aim of this paper is to present the numerous measurements performed during this second period of the experimental program: variation of water content, local and global deformations and deflection of the beams. Relevant experimental evidences are shown on the effect of late changes of moisture conditions on the deformation of ASR-damaged concrete and calculations bring quantitative explanations of the observed behaviour of the reactive beams. Finally, the authors conclude on the way of considering the moisture effect on ASR-induced strains during the life of a possibly ASR-affected structure.

* Corresponding author.
E-mail address: multon@insa-toulouse.fr (S. Multon).

0008-8846/$ – see front matter © 2010 Elsevier Ltd. All rights reserved.
doi:10.1016/j.cemconres.2010.01.011

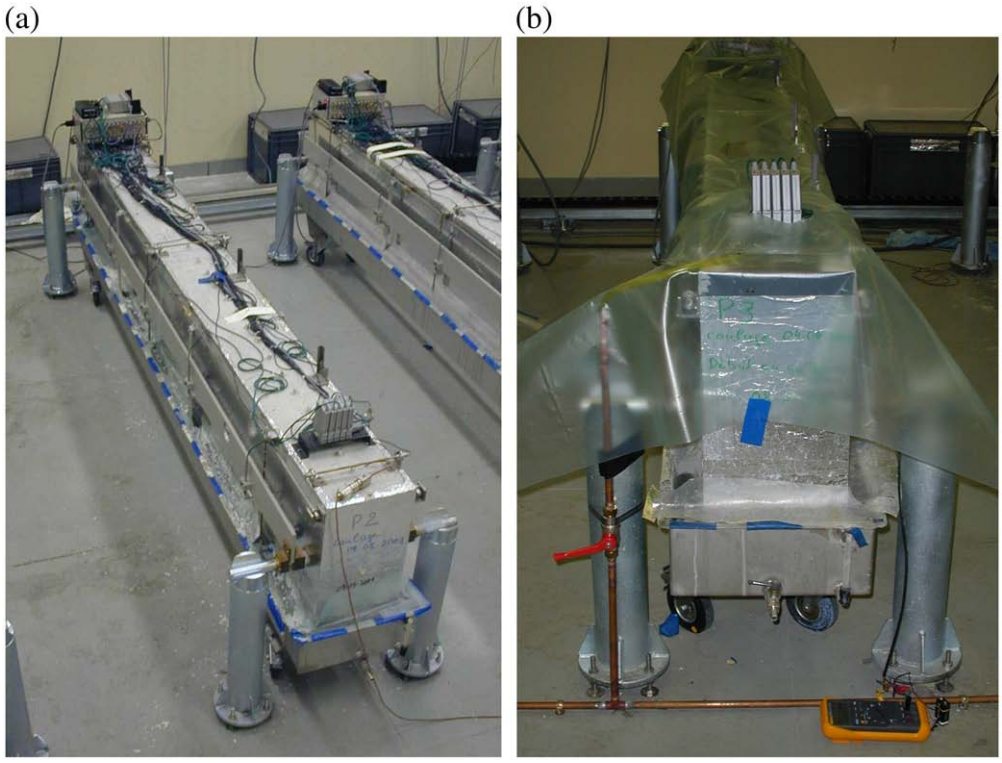

Fig. 1. 3 m-long beam specimen during the drying phase (a) and during the 'late water supply' phase (b).

2. Modification of moisture conditions on ASR-affected specimens

The consequences of change of moisture conditions on ASR-affected specimens are studied. The concrete cylinders first described hereafter are free of external loading (except due to the moisture gradient between the surface and the core of the specimens). The aim is to understand the mechanism of deformations (expansion or shrinkage) at the scale of the material before trying to understand the consequences on structures in the next part.

2.1. Late water supply for specimens already damaged by ASR

2.1.1. Experimental conditions

In order to determine the behaviour of ASR gel submitted to late water supply, specimens (consisting in 32 cm high, 16 cm in diameter cylinders for the measurement along the casting direction and 28 cm high, 14 cm on side prisms for the measurement perpendicular to the casting direction) kept at 38 °C during 676 days either in air at 100% RH or under watertight aluminium, were immersed in water at 38 °C. Free ASR expansions are anisotropic [21–25]. Therefore, strain measurements were carried out in two directions with respect to the casting direction: along the casting direction and perpendicular to it [3]. The mass variations and deformations of specimens submitted to late water supply are plotted in Figs. 3 and 4.

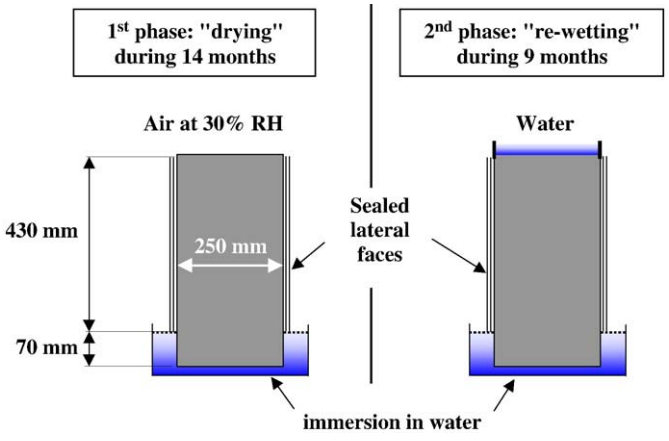

Fig. 2. Moisture conditions of the beams.

2.1.2. Experimental results

For all the specimens, ASR expansions appeared as stabilized before the late water supply. The late water supply caused supplementary expansions even for specimens kept in air at 100% RH before the water supply (Fig. 3). The time evolution of expansions of these specimens can be compared to ASR expansions of specimens kept in water at 38 °C after the 28 curing days (Figs. 3, 4). Measurements on specimens kept in water were performed during 680 days, but deformations were stabilized when measurements stopped. Thus it is considered, here, that deformations of these specimens were constant and equal to deformations measured at the last time-step between 680 and 1000 days.

Mass variation of specimens immersed at 676 days reached in about 80 days the mass variation measured on specimens always kept in water (Figs. 3, 4). The time evolution of the expansions appears to be slower than the mass variation. Therefore, the absorption of water appears not to be the only phenomenon driving the new expansions. In the first days, large deformations were measured. Then, deformations kept on increasing and were almost stabilized 300 days after the beginning of water supply. ASR gel already produced in the first conditions could have swelled in the first days after the late water supply, which would explain the large deformations. However, the chemical reaction could have been stopped by lack of water in some specimens (negative mass variation—aluminium was not perfectly watertight [2]). In these specimens, the water supply can be the cause of the formation of new ASR gel. Large water supply can thus always

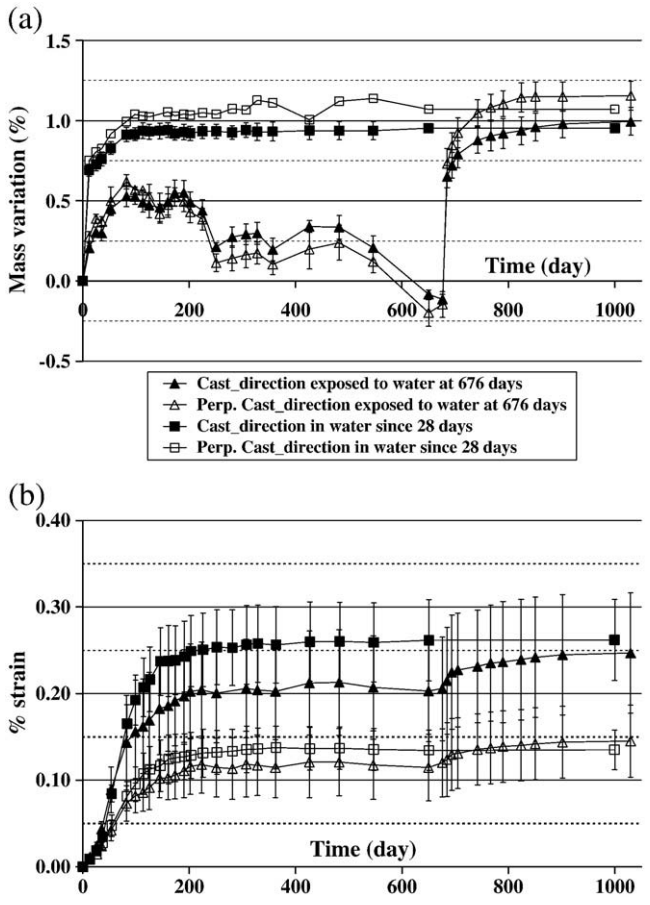

Fig. 3. Mass variations (a) and strains (b) measured on specimens (32 cm high, 16 cm in diameter cylinders and 28 cm high, 14 cm on side prisms) kept in air at 100% RH during 676 days before being submitted to a late water supply.

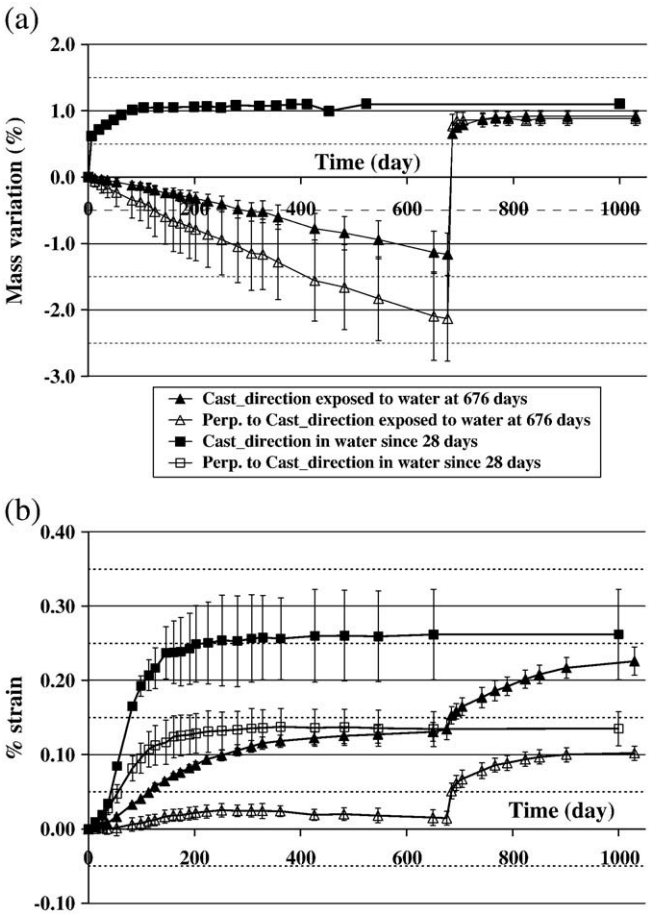

Fig. 4. Mass variations (a) and strains (b) measured on specimens (32 cm high, 16 cm in diameter cylinders and 28 cm high, 14 cm on side prisms) kept under watertight aluminium during 676 days before being submitted to a late water supply.

cause new ASR expansions if the conditions of moisture were not high enough to produce the maximal expansions.

2.2. Drying shrinkage of concrete already damaged by ASR

2.2.1. Experimental conditions

The behaviour of concrete already damaged by ASR is considered under drying conditions, in order to evaluate the shrinkage strains of such concrete and verify if ASR-damaged concrete exhibits more or less shrinkage than a sound concrete. After 28 curing days and 676 days of conservation in water, 32 cm high, 16 cm in diameter cylinders were placed in a 30% RH environment.

2.2.2. Experimental results

All the specimens show the same response to the new conditions (Fig. 5): large loss of mass (about 4% in mass variation) and drying shrinkage (0.05% i.e. 500 μm/m). In order to quantify the modification of the behaviour of the concrete due to previous ASR damage, the strains of the ASR-affected specimens are compared to specimens submitted to the same drying conditions 28 days after the end of the curing period. Fig. 6 shows that both the mass variations and the strains due to drying at 30% RH are perfectly the same for sound concrete as for ASR-damaged concrete. The shrinkage strains had the same kinetics and range whatever the conditions of possible ASR damage and the direction of measurements. The ASR gels and induced cracks did not modify the shrinkage amplitude. Thus, even under severe drying conditions (38 °C and 30% RH), the shrinkage cannot balance the ASR expansions and large irreversible expansions remain observed.

2.3. Conclusion on the effect of the moisture conditions at the material scale

The experimentations carried out on small-scale specimens showed that the ASR does not modify the reversible behaviour of the damaged concrete with respect to moisture-induced strains. Moreover, the ASR deformation appears to be permanent and cumulative if water is supplied. Therefore, special care must be performed when cores are drilled from damaged structures to carry out expansion residual tests. Indeed, a part of the residual expansion can occur between the drilling time and the beginning of the expansion measurements. The cores should be sealed in order to stop any moisture transfer and the residual expansion tests should begin as soon as possible in order to avoid neglecting a certain part of ASR expansions.

3. Structural effects of a late water supply in ASR-damaged beams

3.1. Experimental program

ASR-structural effects have been studied under controlled laboratory conditions in monitoring the evolution of 3 reactive plain or reinforced concrete 3 m-long beams and 2 nonreactive companion specimens (Figs. 1, 7, Table 1), submitted to intense moisture gradient in the height of the beams [3,4]. Therefore the variations in ASR progress caused significant differential expansions and deflections. Realization of controlled moisture gradients within ASR-damaged structures was one original feature of this program. After 28 days curing at 20 °C under aluminium sealing, the 0.25 m–thick 0.5 m-high

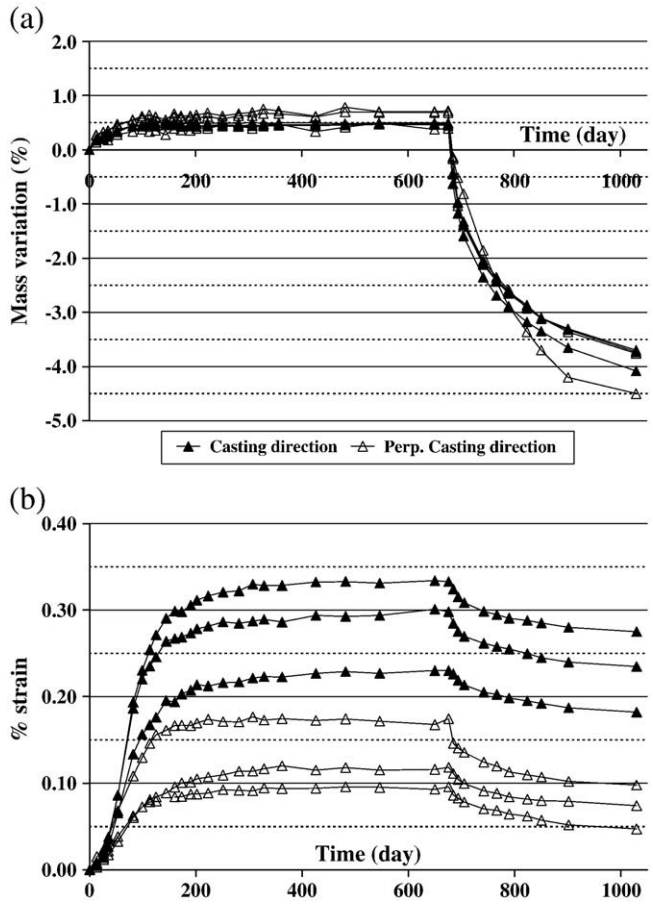

Fig. 5. Mass variations (a) and strains (b) measured on specimens (32 cm high, 16 cm in diameter cylinders) kept in water during 676 days before being submitted to drying at 30% RH.

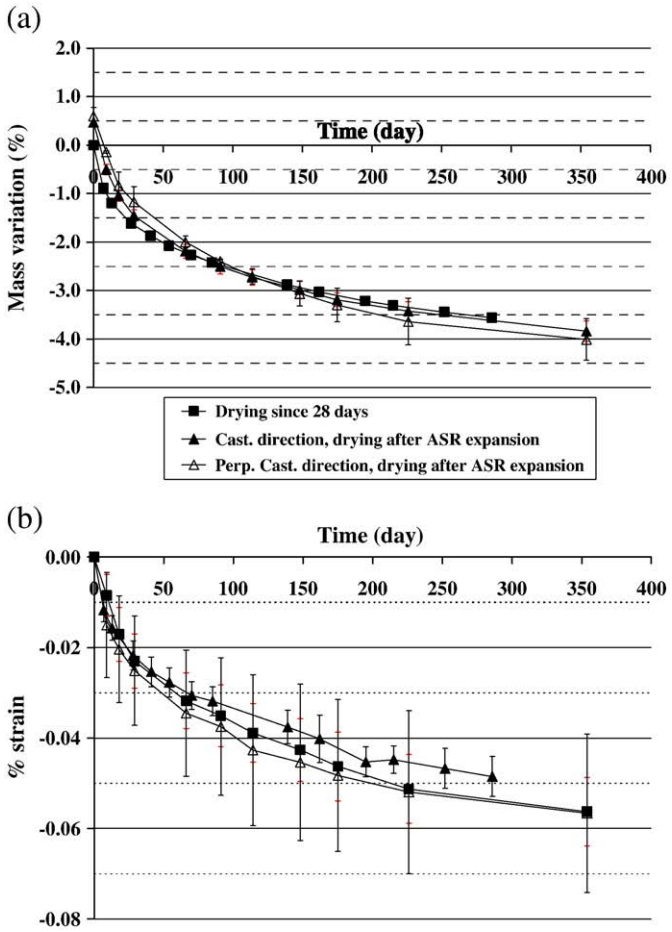

Fig. 6. Mass variations (a) and strains (b) measured on specimens (32 cm high, 16 cm in diameter cylinders) kept in air at 30% RH.

beams were placed in a controlled environment at 38 °C in order to accelerate ASR development (Fig. 2). The beams were placed on simple supports along the geometrical mid-height, with a 2.80 m-span. The lower face of the beams was immersed in water so that the lower part, 0.07 m high, is permanently wet and capillary absorption can take place upwards (Fig. 2). First, the upper face was in contact with air at 30% relative humidity (RH), so that drying can take place from this face downwards (Fig. 2). After 14 months drying the top surface was submitted for 9 further months to permanent water supply (Fig. 2) so that previously stopped ASR expansion could develop again. All the beams were submitted to the same environmental history. Fig. 8 shows the cracking pattern of the upper faces of the three reactive beams. During the first phase, transverse cracks appeared on the three beams. During the second phase, the direction of the cracks was mainly longitudinal for the plain reactive beam *B1*. For the two reinforced beams, some cracks are longitudinal; however the global patterns look like map cracking.

3.2. Moisture distribution in concrete beams

The effect of imposed water supply on reactive and companion beams was quantified using three complementary techniques, so that water diffusion in both types of concrete can be precisely evaluated: capacitive humidity sensors, a specifically-designed dynamometric ring allowing to weigh the global mass variations, and a specifically-adapted gammadensitometry automated device, leading to directly monitoring the drying / rewetting profile in the upper part [2,26,27]. The hydric environment leads to similar global weight losses with time for all beams during the first phase whatever the development of ASR [2,26,27]. The mass losses due to drying can be evaluated by the gammadensitometry device from the upper face to 0.30 m downwards (Fig. 9-a). In the lower part, the depth of water penetration in unsaturated ASR-damaged concrete can be assumed as proportional to the square root of time [27] as for usual concrete [28–30]. This penetration appears not to be affected by ASR, and the mean sorptivity calculated in the lower part of the beams is about 5.8E−3 m day$^{-1/2}$ [27]. After the late water supply, water movements can be analyzed as consisting of two steps. First, analysis of gammadensitometry measurements showed that concrete recovers quasi-instantaneously moisture conditions measured after the 28 curing days [2]; then the penetration of water can be modelled as proportional to the square root of time (Fig. 9-b). After the first 14 months, the reactive beams were significantly damaged, and transversal large cracks had appeared on the upper faces. The sorptivity values determined in the upper part of the beams were different of those determined in the lower part and the scattering of sorptivity between the concrete of the five beams was larger (sorptivity of about 4.3E−3 m day$^{-1/2}$ for the plain and reactive beam *B1*; 7.0E−3 m day$^{-1/2}$ for the reinforced beam *B3* and 15.5E−3 m day$^{-1/2}$ for the reinforced beam *B4*). The differences between the three reactive beams can be explained by the presence of cracks on the upper face of the beams: only 3 transverse cracks for *B1*, 9 for *B3* and 15 for *B4* (Fig. 8). Thus, the more intense the cracking of the beam, the faster is the water transfer. Mean profiles of mass variations along the depth of the five beams are plotted in Fig. 9 (the absolute standard deviation of mass variations on the five beams is about 1%). These profiles are necessary to analyze and evaluate the structural behaviour of the beams.

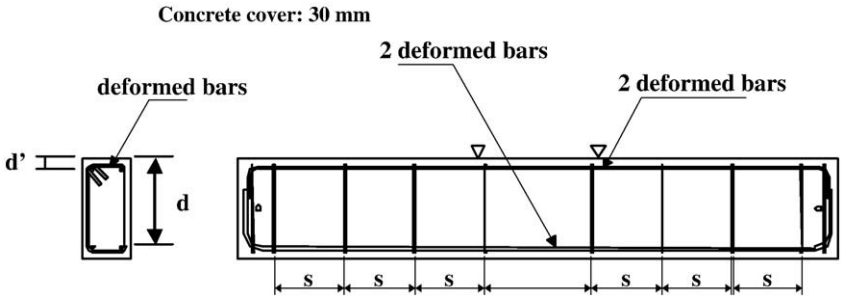

Fig. 7. Elevation and cross-section of the reinforced concrete beams.

3.3. Transverse and vertical deformations

Precision and statistical significance in quantifying the structural deformations were obtained using redundant instrumentation, based on vibrating wire sensors (85 mm-gauge length) located at different depths (0.08, 0.17, 0.27 and 0.37 m from the upper face) in the three directions (transverse, vertical and longitudinal) [3]. In the current section, the strains measured in the transverse and vertical directions of the two plain beams *B1* and *B2* are described. Along the vertical direction, strains are ideally free of applied vertical stresses, and directly reflect the influence of local moisture conditions on ASR expansion.

During the first 14 months, the range of vertical strain was observed as directly related to water supply, both for reactive and nonreactive plain beams (Figs. 10-a and 11-a). For the nonreactive beam, shrinkage was measured at the depth of 0.08 and 0.17 m, and expansions due to water absorption at 0.27 and 0.37 m (Fig. 11). For the reactive beam, the closer the water supply concrete was, the larger were the ASR expansions (Fig. 10). At 0.08 m, ASR expansions were smaller than in the lower part due to the drying effect, but ASR appeared not to be stopped. After the late water supply, strains in the nonreactive beam increased quickly, to reach positive values in almost the whole beam (physical expansion due to water absorption). For the reactive beam, ASR expansions increased a lot, as soon as the late water supply occurred. The late swellings are particularly intense between the upper face and the depth of 0.08 m. At the depth of 0.17 m, ASR expansions appear to be only slightly accelerated. Below this depth, the strains keep on increasing with the same expansion rate. These measurements are consistent with measurements on cylinders exposed to late water supply, which exhibit fast late expansions as soon as water is supplied. These results are only presented for the plain beams because for reinforced beams the stirrups induce local disturbance, leading to hardly significant effects on vertical and transverse deformations [2] as already observed during the drying phase [3].

3.4. Longitudinal deformations

3.4.1. Longitudinal deformation of concrete beams

Previous analysis of the first phase of drying [3] has shown that the longitudinal behaviour of the beams can be summarized by only two data, namely, the mean relative length variation, approximated by the direct measurement of the 3 m long vibrating wire sensors at a depth of 0.23 m (near neutral axis—Fig. 12), and the mean curvature (experimentally quantified by the deflection at mid-span—Fig. 13).

During the first phase, the predominance of the ASR-induced strains in the bottom part compared to shrinkage in the upper part drove to large curvature and thus important deflection for the reactive plain beam *B1* (Fig. 13). The measurements on the nonreactive plain concrete beam B2 showed a smaller deflection. The curvature of the plane sections led to mid-span deflections of 5.4 mm for *B1* and 1.0 mm for *B2* at the age of about 420 days. For nonreactive beams, the reinforcement had no visible influence due to relatively low strains (comparison of *B5* with *B2*). For reactive beams, the comparison of the strains and deflections of the beams *B3* and *B4* with *B1* emphasizes the significant effect of the reinforcement on ASR-induced strains. After 14 months, the length relative variation at the depth of 0.23 m was approximately 0.08% for *B3* and 0.04% for *B4*, to be compared with 0.11% for *B1*. The deflection reached only 1.1 and 0.3 mm for *B3* and *B4*, respectively, instead of 5.4 mm for *B1*.

The late water supply had the same effect for the five beams: increase of mean strains and reduction of deflections (and even inversion of the deflection for the two reactive and reinforced beams). For the two nonreactive beams, the strains become equal to zero but the deflections stay slightly negative (about 0.5 mm). For the plain reactive beam, the curvature decreased but the deflection variation remained below 2 mm and the deflection stayed largely negative even when the phenomena seemed stabilized. For the reactive and reinforced beams, the deflections became positive which indicates that the strains in the upper part were larger than the strains in the bottom. It can be partly explained by the dissymmetry of the reinforcement. The structural analysis detailed hereafter shall especially help in understanding the global behaviour of the three reactive beams.

Table 1
Beams details (see Fig. 7).

Beam	Concrete	Lower reinforcement	Upper reinforcement	Stirrups
B1	Reactive	None	None	None
B2	Nonreactive	None	None	None
B3	Reactive	2 ribbed #16 bars (d = 0.45 m)	2 rib. #10 bars (d' = 0.045 m)	#8, s = 0.35 m
B4	Reactive	2 ribbed #32 bars (d = 0.42 m)	2 rib. #20 bars (d' = 0.050 m)	#12, s = 0.20 m
B5	Nonreactive	2 ribbed #16 bars (d = 0.45 m)	2 rib. #10 bars (d' = 0.045 m)	#8, s = 0.35 m

3.4.2. Moisture-dependent ASR-induced strains

In order to analyze the longitudinal behaviour of the beams, mechanical calculations have been carried out according to the Strength of Materials theory. This relies on the assumption that cross-sections remain plane, which is quite well verified during the two phases [2,3]. The Strength of Materials theory can thus be applied in order to check the possibility of using ASR expansions measured on specimens, as direct input prescribed chemical strains. A simplified profile of imposed strains was adopted so that analytic computations could be carried out. Such an analysis has already been performed for the nonreactive beam [4] and for the first period of drying of the reactive beams [5]. It is presently applied to analyze the structural behaviour of the three reactive beams after the late water supply. Previous analysis has shown that, for specimens kept in an environment with a constant temperature, the two main parameters which affect ASR-induced strains are the moisture content with concrete and the mechanical stresses applied on the material. The chemical imposed strain profiles were deduced from the moisture

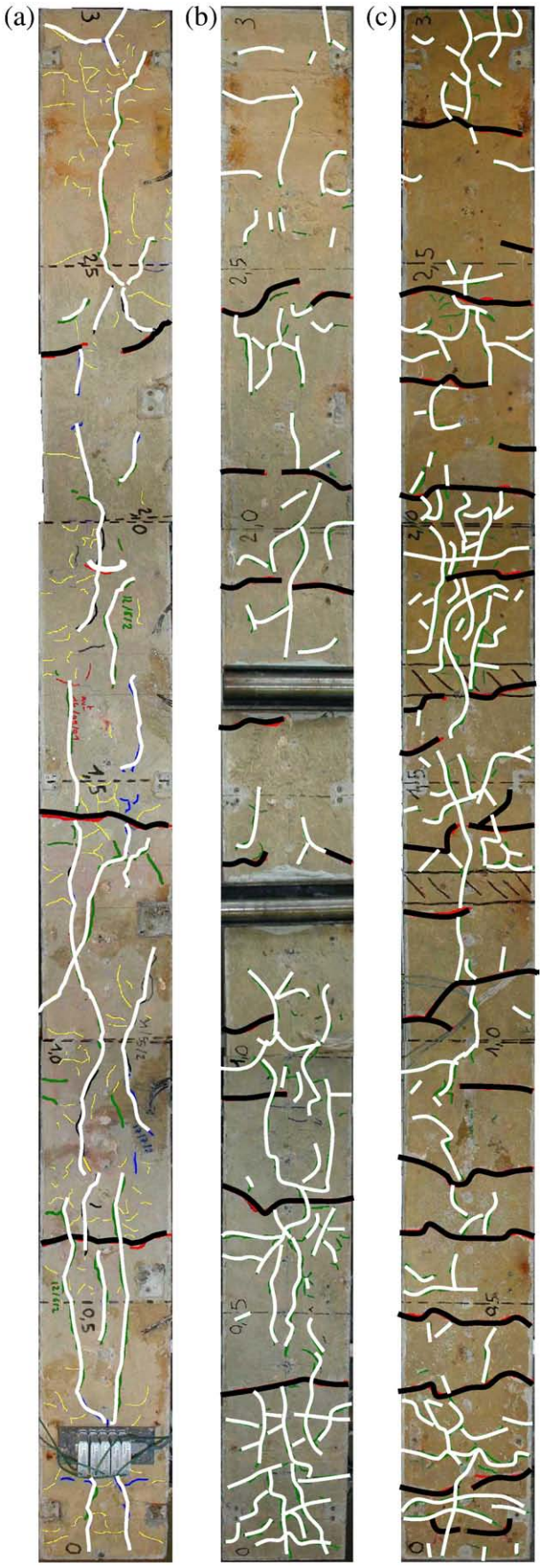

Fig. 8. Upper face of beams *B1* (a), *B3* (b) and *B4* (c), in black: cracks appeared during drying—first 14 months—in white: cracks appeared after the late water supply.

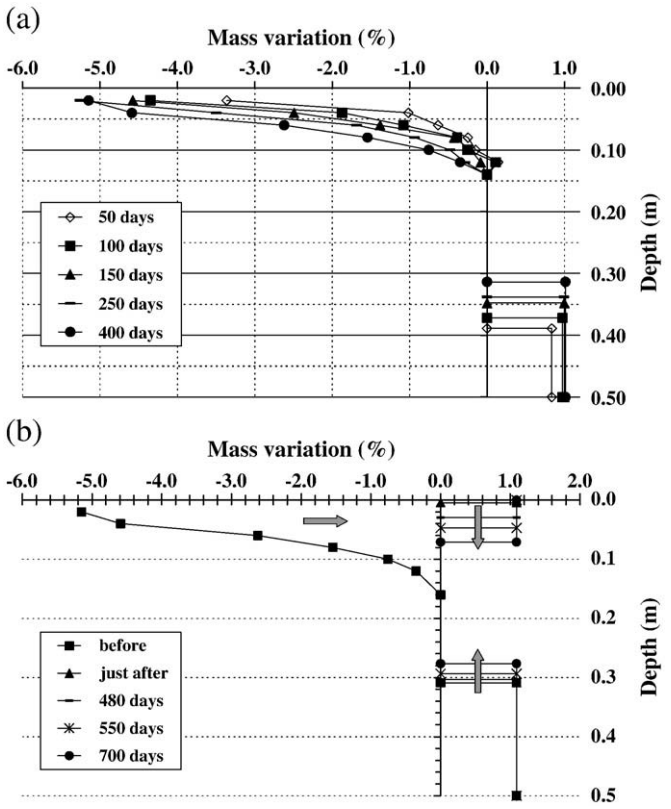

Fig. 9. Moisture distribution in concrete beams (average values) during the first 14 months (a) and after the late water supply (b).

profile (Fig. 9) and from the measurement of ASR-induced expansions performed on cylindrical specimens kept in water and under watertight aluminium. Concerning the influence of applied stresses, the conclusions drawn from the analysis performed on specimens submitted to large stresses and restraint [6] and on the three reactive beams during the first 14 months in [5], were that the imposed strains had to be taken as:

- isotropic in the part only concerned by shrinkage,
- isotropic in the part submitted to small stresses, i.e. for unreinforced part of the beams in case of no visible cracking,
- anisotropic in the cracked part of the plain beams or for the reinforced beams: with larger imposed strains in the direction perpendicular to cracks and with smaller imposed strains in the direction parallel to steel reinforcement.

During the first phase of drying, it has been validated that the imposed strains should be taken with consideration of the direct influence of moisture conditions [5]. After the late water supply, the same method is used; the assumptions on ASR imposed strains in the upper part of the beams have been divided into two steps as for the analysis of the moisture in the beam:

- In the first step, concrete in the upper part of the beam is considered to recover instantaneously the moisture conditions measured after the 28 curing days. Thus, the ASR imposed strains are assumed to be related to the same moisture conditions that concrete without mass losses ($\varepsilon_{\delta m=0}$). ASR expansions deduced from deformations measured on specimens kept under watertight aluminium are thus assumed in the upper part (Figs. 14 and 15). These ASR expansions start as soon as the upper face is exposed to water supply (t_{LWS}: time-step corresponding to the late water supply).

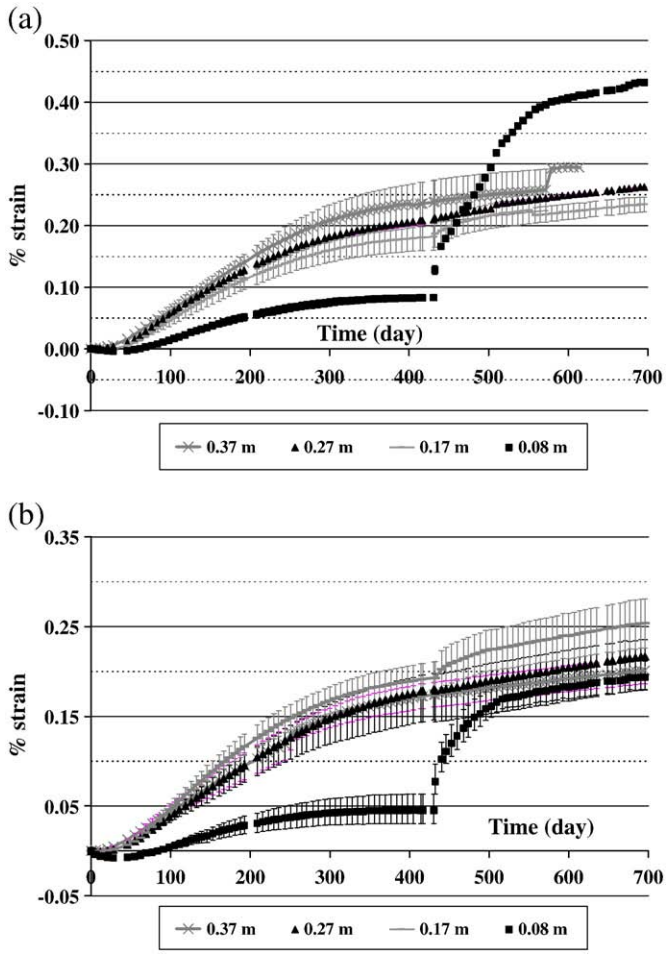

Fig. 10. Vertical (a) and transverse (b) strains of the plain reactive beam B1 measured at four depths (0.08, 0.17, 0.27 and 0.37 m from the upper face), the late water supply occurs after the measurement at 431 days.

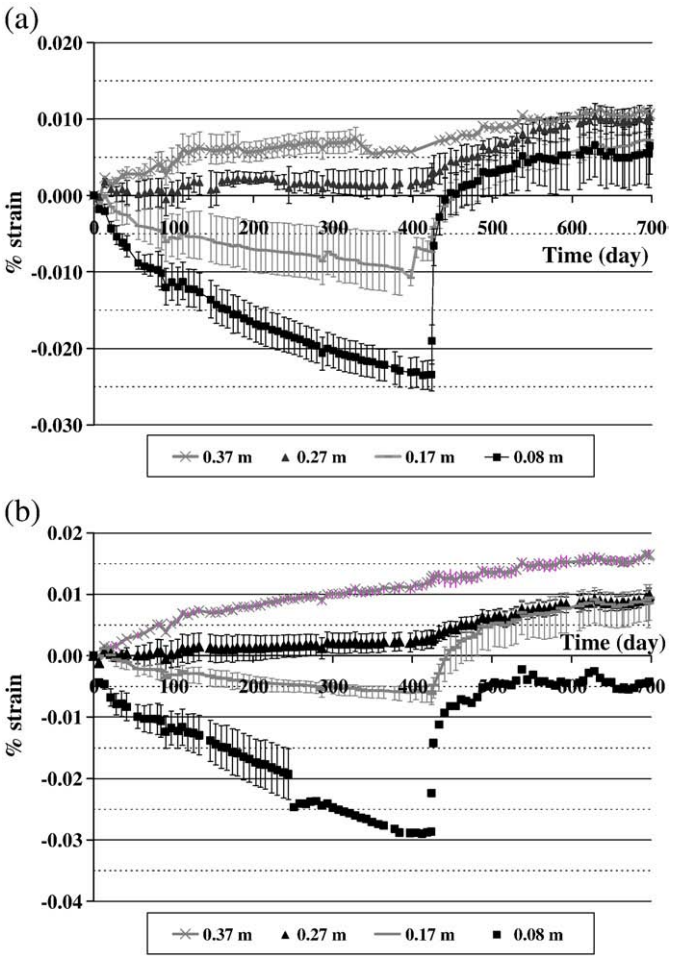

Fig. 11. Vertical (a) and transverse (b) strains of the plain nonreactive beam B2 measured at four depths (0.08, 0.17, 0.27 and 0.37 m from the upper face), the late water supply occurs after the measurement at 424 days.

– In the second step, concrete in the upper part becomes saturated by the penetration of the water front. The depth reached by water in this imbibition process can be evaluated as following a time evolution according to the square root of time. The ASR imposed strains in the part of concrete reached by the water front (ε_{wat}) are derived from the specimens kept in water (Figs. 15 and 16—t_{wat}: time-step corresponding to the instant when water saturation reaches this part of the concrete).

In the lower part, the moisture distribution pattern did not change, the water penetration in the lower part kept on with the same time evolution as in the analysis of the first part [5].

The behaviour of the three reactive beams has been evaluated from the combination of the "material data" (obtained on specimens) and of the "moisture data" as detailed above.

3.4.3. Structural analysis

3.4.3.1. Mechanical equations. The ASR-affected beams are submitted to chemical swellings considered as imposed strains. Since neither external bending moment nor axial load is applied, and neglecting the self-weight, the two equations of mechanical equilibrium of each cross-section read:

$$\begin{cases} N(t) = \int_0^h \sigma(t,z).w.dz + A\sigma_s(t,d) + A'\sigma_s\left(t,d'\right) = 0 \\ M_f(t) = \int_0^h \sigma(t,z).z.w.dz + dA\sigma_s(t,d) + d'A'\sigma_s\left(t,d'\right) = 0 \end{cases} \quad (1)$$

whatever is the time t considered, with N and M_b, the axial force and the bending moment in the cross-section, σ, the stress in the concrete, σ_s, the stress in the steel reinforcement, h and w, the height and the width of the beam, A and A', the areas of the lower and upper steel reinforcement, d and d', the distances between the center of gravity of the lower and upper steel reinforcement and the upper face of the beam, respectively. If chemo-elasticity applies [5], the longitudinal stresses in a cross-section of a beam subject to imposed strain can be written:

$$\sigma(t,z) = E\cdot\left(\varepsilon(t,z) - \varepsilon_{imp}(t,z)\right) \quad (2)$$

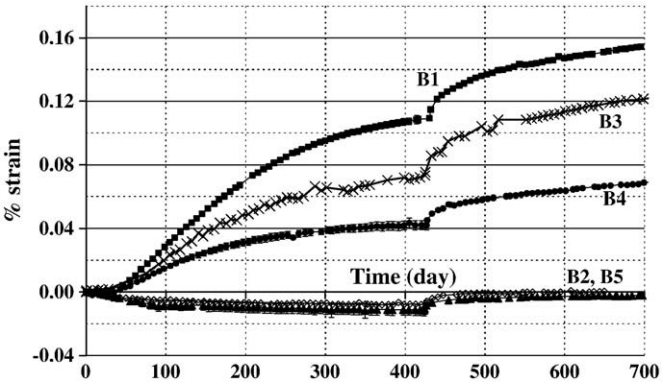

Fig. 12. Overall longitudinal deformation at 0.23 m for the five beams.

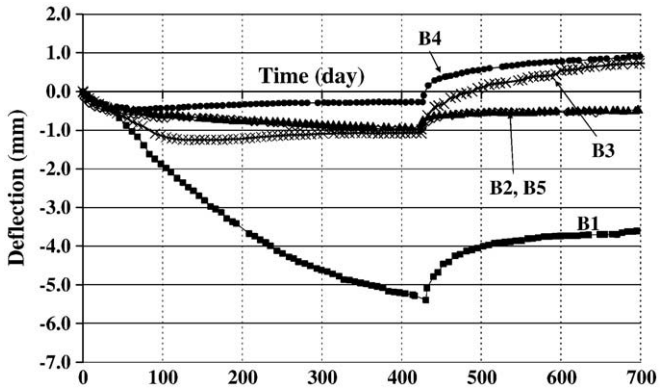

Fig. 13. Deflection at mid-span for the five beams.

with E, the Young's Modulus of the reactive concrete, $\varepsilon(z)$, the longitudinal strain and $\varepsilon_{imp}(z)$, the chemically-induced longitudinal strain according to water supply and stress conditions.

Moreover, the assumption that cross-sections remain plane allows representing the longitudinal strains profile by a straight-line:

$$\varepsilon(z) = \varepsilon_0'.z + \varepsilon_0 \quad (3)$$

Therefore, integration of equilibrium equations of the section leads to two equations with two unknown factors (ε'_0 and ε_0).

These equations have been solved for every time-step corresponding to experimental measurement. Since chemically-induced expansions have been identified with a rather large scatter (Figs. 3 and 4), calculations were based on mean expansions, however standard deviation of calculations has been evaluated [5]. The uncertainty of the calculations comes both from uncertainty of the moisture distribution and from the scatter in the ASR-induced deformations measured on the specimens. It can be assessed by the derivation of Eq. (3) [5].

3.4.3.2. Plain and reactive beam. In order to analyze the capacity of calculations to predict the behaviour of the plain and reactive beam *B1*, calculated longitudinal strain at the depth of 0.23 m and deflections at mid-span, as well as corresponding measured values have been plotted in Fig. 17 (calculation 1). As observed in Fig. 17, the average deformation at the depth of 0.23 m is quite well evaluated by calculation 1 (absolute mean quadratic deviation assessed between calculated and measured values is about 0.005%). At the opposite, the deflection at mid-span is significantly underestimated (mean quadratic deviation between calculated and measured values is about 1.0 mm). The difference between calculated and measured deflections can be explained by large compressive stresses, induced by the late water supply. Indeed, in these conditions, compressive stresses of about 10 MPa are evaluated in the upper part of the beams only 70 days after the late water supply. Such compressive stresses cause large reduction of ASR-induced strains along the compressed direction and the "expansion transfer" shall have occurred along perpendicular directions [5,6]. Therefore calculation 2 has been computed with imposed strains reduced in the whole upper part using a simplified first approach reduction factor. Imposed strains due to the late water supply become:

$$\varepsilon_{imp} = \alpha.\varepsilon_{\delta m=0}(t - t_{LWS}) \quad (4)$$

in the whole upper part concerned with the late water supply, and

$$\varepsilon_{imp} = \alpha.(\varepsilon_{\delta m=0}(t_{wat} - t_{LWS}) + \varepsilon_{wat}(t - t_{LWS})) \quad (5)$$

in the part of concrete reached by water penetration. α is the reduction factor which takes into account reduction due to compressive stresses already used to analyze the behaviour of the reinforced beams during the period of drying [5]. Therefore, the imposed expansions are anisotropic. The reduction factor used in the analysis of this experiment lies between 0.2 and 0.45 according to the studied beam; which can be compared to the reduction factor of about 0.35 obtained on specimens for compressive stresses of 10 MPa for the same concrete [5].

The global reduction factor has been evaluated to obtain calculated deflection at mid-span close to measured one (Fig. 17-b). The aim of these calculations was not to be predictive but to explain the behaviour of the plain and reactive beam due to the late water supply. With a reduction factor of about 0.4 (which represents 60% reduction of ASR-induced strains), the behaviour of the beam can be reproduced (the mean quadratic deviation between calculated and measured values is about 0.15 mm for deflection and about 0.015% for strain). Evaluation of the mean axial expansion at the depth of 0.23 m is not as good as previously calculated; however, the global calculated behaviour appears to be more representative of the experimentally observed behaviour. This 60% reduction of ASR-induced strain is quite close to the calculated reduction on cylindrical specimens submitted to a 10 MPa axial compressive stress [6]. Therefore, the result is quite consistent with previous results. The development of large compressive stresses in the upper part of the beam *B1* which implies the reduction of the imposed strains in the longitudinal direction causes larger induced strains in the perpendicular directions. The consequences of such "transfer" can be observed on the crack pattern of the upper face of the beam (Fig. 8) with major longitudinal cracks due to large transverse expansions. In this rough approach, calculations have been done using a global coefficient while the reduction should be calculated at every depth of the beam according to the compressive stress. However, a model recently developed [14] analyzed this same experiment with a predictive approach. It confirmed the anisotropy of

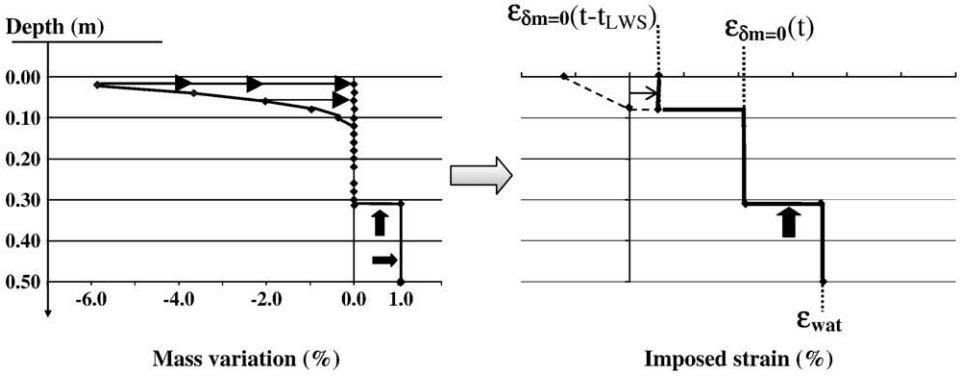

Fig. 14. Imposed strains during the first stage following the late water supply (t_{LWS}: time-step corresponding to the late water supply).

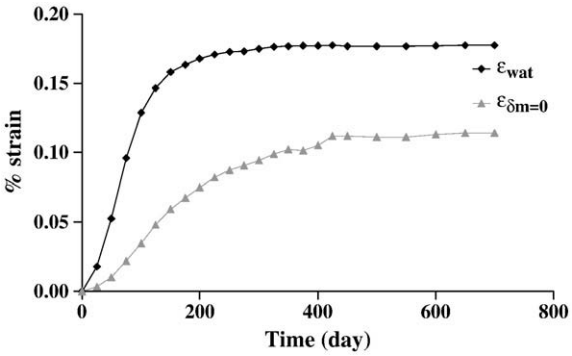

Fig. 15. Imposed strains for concrete kept in water and for concrete without mass variation.

expansions (via an anisotropic damage) in the upper part of the beam in order to predict the behaviour of the beam.

As a conclusion of this structural analysis, longitudinal behaviour of the plain and reactive beam *B1* was successfully explained during the whole exposure process, and especially during the second phase by the development of ASR-induced strains in the upper part of concrete due to the late water supply. These strains cause longitudinal compressive stresses which imply reduction of ASR expansions in the longitudinal direction and large longitudinal cracks. It has turned out that the stress-induced anisotropy of ASR expansions has to be taken into account for a correct prediction.

3.4.3.3. Reinforced and reactive beams. The same analysis has been carried out on the reactive and reinforced beams *B3* and *B4*. For these calculations, global reduction factors have been taken into account in the lower part of the beams due to lower reinforcement. The factors have been taken equal to those determined during the first period of drying [5]. Like in the previous part, the two calculations have been performed: Calculation 1, without reduction factors on the imposed strains in the upper part, and Calculation 2 with reduction factors on the imposed strains in the upper part. Calculation 1 gives a good result for the mean deformation of the beam *B3*; while the deflections calculated for the two reinforced beams are very different from the measurements (Figs. 18 and 19). Calculation 2 leads to better results, except for the longitudinal deformation which is slightly underestimated. The approach used here appears to be too rough to represent all the phenomena occurring in the concrete and to be able to reproduce perfectly the structural behaviour. However, it emphasizes the requirements of correctly taking into account the stress-induced anisotropy to predict the behaviour of the beams. The reduction is due to compressive stresses (about 5 MPa), caused by the late water supply and by the presence of reinforcement. Reduction factors of about 55% and 80% in the upper part of the beams *B3* and *B4*, respectively, have turned out necessary to roughly obtain mean strains and deflection at mid-span measured on the beams (Figs. 18 and 19). The reduction for the beam with low reinforcement *B3* is slightly lower than the reduction for the plain beam *B2*. This is consistent with the value of compressive stresses calculated without taking into account the stress-induced modification of the expansions: about 8 MPa for the beam *B3* after 125 days and about 12 MPa after 75 days for the beam *B4*.

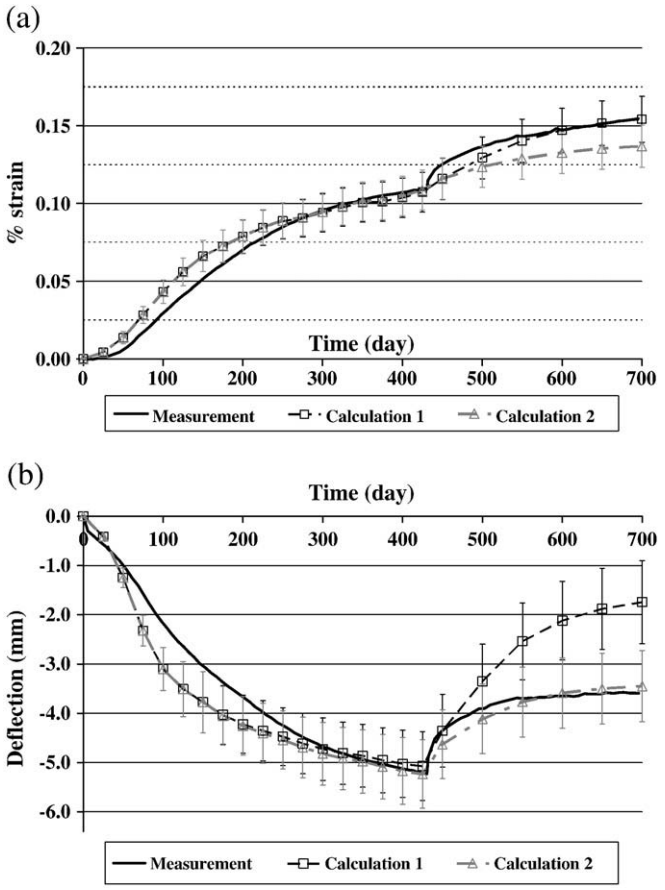

Fig. 17. Comparison of calculation and measurements: overall longitudinal deformation at 0.23 m (a) and deflection at mid-span (b) of the plain reactive beam B1.

During the period following the late water supply, the additional expansions cause a slight decrease of the tensile stresses in the lower

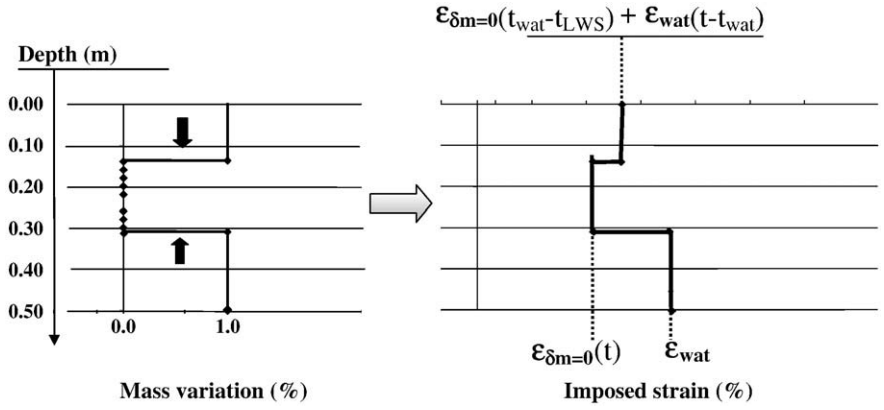

Fig. 16. Imposed strains during the second stage following the late water supply (t_{wat}: time when concrete is reached by the water penetration).

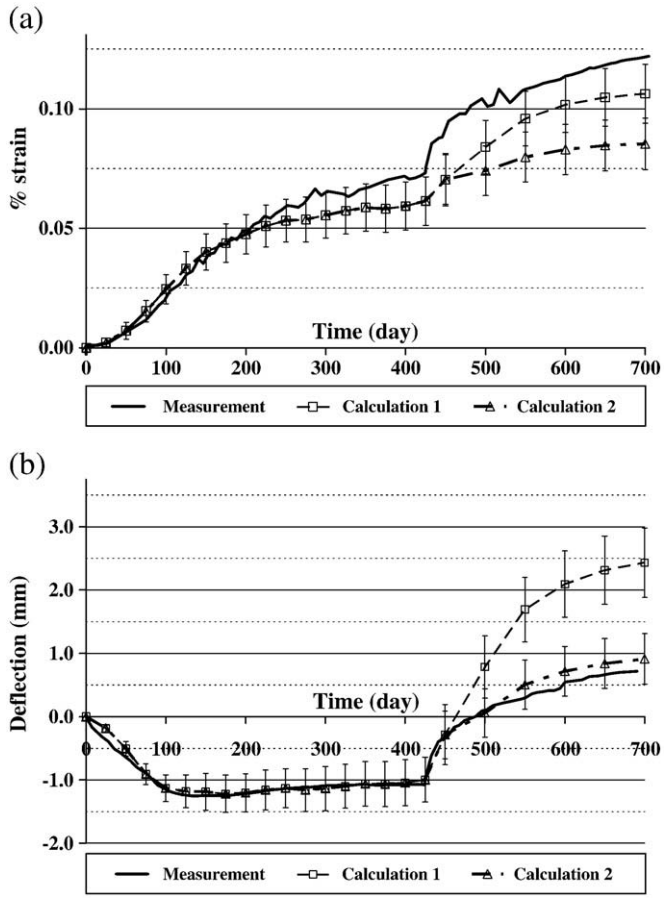

Fig. 18. Comparison of calculation and measurements: overall longitudinal deformation at 0.23 m (a) and deflection at mid-span (b) of the reinforced reactive beam *B3*.

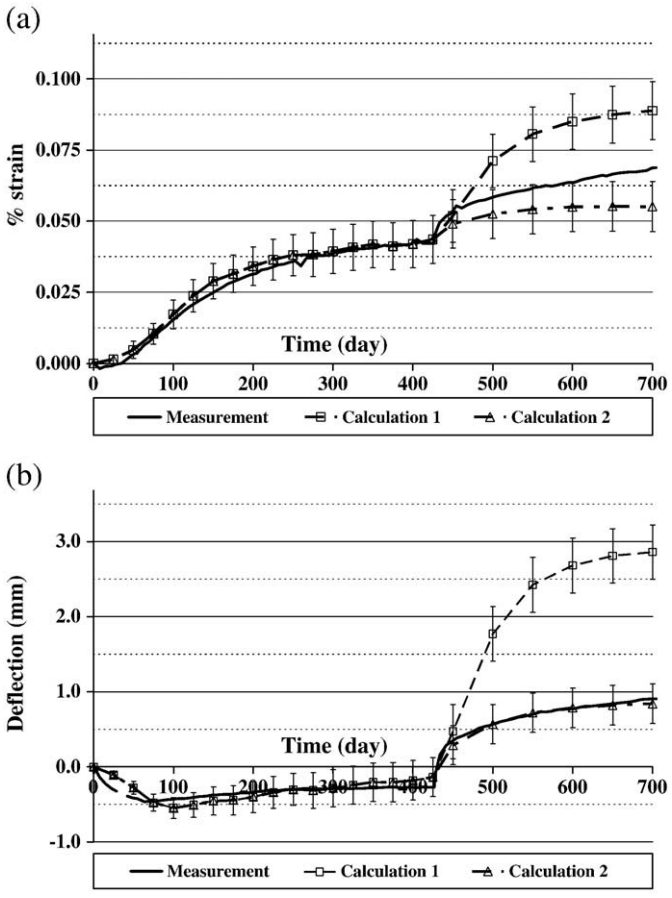

Fig. 19. Comparison of calculation and measurements: overall longitudinal deformation at 0.23 m (a) and deflection at mid-span (b) of the reinforced reactive beam *B4*.

reinforcement steels: 130 and 80 MPa in the beams *B3* and *B4* at 700 days, while stresses were equal to 160 and 100 MPa at the end of the drying period [5], and an increase of the tensile stresses in the upper reinforcement steels up to 200 and 140 MPa for *B3* and *B4* respectively.

The calculations performed in this paper bring quantitative explanation of the observed behaviour of the two reinforced and reactive beams. It also turns out necessary to introduce a reduction factor in the compressed parts of the beams. Therefore, it is confirmed that structural models used to reassess damaged structures shall take into account this anisotropy of expansion due to stresses.

4. Conclusion

Characterization of ASR-induced expansions due to modification of moisture conditions has been carried out on specimens and structures. Measurements on cylinders have shown that late water supply causes new ASR expansions in concrete if the maximal potential expansion has not been reached before due to possible lack of available water. Moreover, these experimentations have shown that the ASR gels do not change the shrinkage potential of the damaged concrete. The amplitude of the drying shrinkage, even in severe conditions (about 0.05% for specimens kept in air at 38 °C and 30% RH), counteracts only slightly the expansion due to ASR in the case of rather reactive concrete (with potential amplitude of about 0.30%).

Characterization of the structural behaviour of plain and reinforced reactive beams analyzed with consideration of the moisture distribution confirms this conclusion. The behaviour of the plain and reactive beam after the late water supply can be explained by two main processes. First, additional ASR expansions occur where saturation was not reached. Secondly, these imposed strains imply large longitudinal compressive stresses, which reduce longitudinal imposed strains and cause the transfer of expansion in directions free of restraint. This analysis based on chemo-mechanical approach has been carried out using the Strength of Materials theory. It validates the assumption of considering ASR expansion as imposed strains directly related to local water supply. It also confirms that the imposed strains have to depend on the stress state of studied structures [5,6,13,31]. However, as shown in the analysis of the behaviour of the plain and reactive beam, in ASR-damaged structures, this stress state is largely influenced by the moisture conditions.

Finally, if water is supplied at anytime of the life of an ASR-damaged structure, ASR gel already produced can rapidly swell. Moreover, the chemical reaction could have been stopped by lack of water in some places of the structure. In this case, the water supply can cause the formation of new ASR gels. Therefore, concrete will develop supplementary ASR expansions as long as the maximum expansion is not reached. This maximum expansion can only be achieved after long-term exposure to moisture. The absorption of water by old gels and the creation of new gels will cause an additional increment of irreversible imposed strains which can be assessed from ASR-affected concrete kept in water. Moisture dependence of the imposed strains should be driven by the saturation degree [10,17]. During this process, periods of drying imply reversible drying shrinkage proportional to the loss of mass, as for nonreactive concrete [4,32]. Relying on this same basis of experimental evidence, different approaches can be considered in order to take into account the effect of the moisture conditions in models [13,18,33,34].

Acknowledgements

The authors are pleased to thank the teams of technicians at LCPC (structures laboratory) who participated in the measurements reported in this paper. They thank S. Prené, H. Tournier, E. Bourdarot, A. Jeanpierre and D. Chauvel (EDF) for their help in analysis and financial support.

References

[1] S. Multon, J.-F. Seignol, E. Bourdarot, A. Jeanpierre, F. Toutlemonde, Effets structuraux de l'alcali-réaction—Apports d'une expérimentation sur éléments de structures à la validation de modèles, Rev. Eur Génie Civ. 9 (2005) 1219–1247.
[2] S. Multon, Evaluation expérimentale et théorique des effets mécaniques de l'alcali-réaction sur des structures modèles, PhD Thesis, University of Marne la Vallée, France, 2003.
[3] S. Multon, J.-F. Seignol, F. Toutlemonde, Structural behavior of concrete beams affected by Alkali-Silica Reaction, ACI Materials Journal 102 (2005) 67–76.
[4] S. Multon, J.-F. Seignol, F. Toutlemonde, Concrete beams submitted to various moisture environments, Struct. Eng. Mech. 22 (2006) 71–83.
[5] S. Multon, J.-F. Seignol, F. Toutlemonde, Chemomechanical assessment of beams damaged by Alkali-Silica Reaction, ASCE, J. Mat. in Civil Eng. 18 (2006) 500–509.
[6] S. Multon, F. Toutlemonde, Effect of applied stresses on alkali-silica reaction induced expansions, Cem. Conc. Res. 36 (2006) 912–920.
[7] P. Léger, P. Cote, R. Tinawi, Finite element analysis of concrete swelling due to alkali-aggregate reaction in dams, Comp. and Struct. 60 (1996) 601–611.
[8] F. Ulm, O. Coussy, L. Kefei, C. Larive, Thermo-chemo-mechanics of ASR expansion in concrete structures, ASCE, J. of Eng. Mech. 126 (2000) 233–242.
[9] K. Li, O. Coussy, Concrete ASR degradation: from material modeling to structure assessment, Concr. Sci. Eng. 4 (2002) 35–46.
[10] S. Poyet, Etude de la dégradation des ouvrages en béton atteints de la réaction alcali-silice: approche expérimentale et modélisation numérique multi-échelle des dégradations dans un environnement hydrochemo-mécanique variable, PhD Thesis, University of Marne la Vallée, France, 2003.
[11] J.-F. Seignol, F. Barbier, S. Multon, F. Toutlemonde, Numerical simulation of ASR affected beams, comparison to experimental data, Proc. 12th Int. Conf. on AAR, Beijing, China, 2004, pp. 198–206.
[12] V. Saouma, L. Perotti, T. Shimpo, Stress analysis of concrete structures subjected to alkali-aggregate reactions, ACI Struct. J. 104 (2007) 532–541.
[13] E. Grimal, A. Sellier, Y. Le Pape, E. Bourdarot, Creep, shrinkage and anisotropic damage in AAR swelling mechanism—part I: a constitutive model, ACI Struct. J. 105 (2008) 227–235.
[14] E. Grimal, A. Sellier, Y. Le Pape, E. Bourdarot, Creep, shrinkage and anisotropic damage in AAR swelling mechanism—part II: identification of model parameters and application, ACI Struct. J. 105 (2008) 236–242.
[15] H. Olafsson, The effect of relative humidity and temperature on alkali expansion of mortar bars, Proc. of the 7th ICAAR, Ottawa, Canada, 1986, pp. 461–465.
[16] T. Kurihara, K. Katawaki, Effects of moisture control and inhibition on alkali silica reaction, Proc. of the 8th ICAAR, Kyoto, Japan, 1989, pp. 629–634.
[17] C. Larive, A. Laplaud, O. Coussy, The role of water in alkali-silica reaction, Proc. of the 11th ICAAR, Quebec, Canada, 2000, pp. 61–70.
[18] S. Poyet, A. Sellier, B. Capra, G. Thèvenin-Foray, J.-M. Torrenti, H. Tournier-Cognon, E. Bourdarot, Influence of water on alkali-silica reaction: experimental study and numerical simulations, ASCE, J. Mat. Civil Eng. 18 (2006) 588–596.
[19] J.-F. Seignol, T.T. Ngo, F. Toutlemonde, Modeling of the coupling between moisture and alkali-silica reaction in concrete, in: Meschke, et al., (Eds.), Computational Modeling of Concrete Structures », Proceedings of Euro-C 2006 conference, Mayrhofen (Austria), Taylor & Francis Group, London, 2006, pp. 639–646.
[20] A. Steffens, K. Li, O. Coussy, Aging approach to water effect on alkali-silica reaction degradation of structures, ASCE J. Eng. Mech. 129 (2003) 50–59.
[21] L.A. Clark, K.E. Ng, Some factors influencing expansion and strength of the SERC/BRE Standard ASR concrete mix, Science and Engineering Research Council, Repair, Maintenance and Operations Conference, London, Great-Britain, 1989 89–94.
[22] A.E. Jones, L.A. Clark, The effects of restraint on ASR expansion of reinforced concrete, Mag. Conc. Res. 48 (1996) 1–13.
[23] G. Ballivy, K. Khayat, C. Gravel, D. Houle, Influence of reinforcement steel on the expansion of concrete affected by Alkali-Aggregate Reaction, Proc. of the 11th ICAAR, Québec, Canada, 2000, pp. 919–928.
[24] C. Larive, M. Joly, O. Coussy, Heterogeneity and anisotropy in ASR-affected concrete—consequences for structural assessment, Proc. of the 11th ICAAR, Québec, Canada, 2000, pp. 969–978.
[25] N. Smaoui, M.A. Bérubé, B. Fournier, B. Bissonnette, "Influence of specimen geometry, direction of casting, and mode of oncrete consolidation on expansion due to ASR", J. Cem., Concr., Aggregates (ASTM) 26 (2) (2004) 58–70.
[26] S. Multon, F. Toutlemonde, Water distribution in concrete beams, Mat. Struct. 37 (2004) 378–386.
[27] S. Multon, E. Merliot, M. Joly, F. Toutlemonde, Water distribution in beams damaged by Alkali-Silica Reaction: global weighing and local gammadensitometry measurements, Mat. Struct. 37 (2004) 282–288.
[28] C. Hall, Water sorptivity of mortars and concretes: a review, Mag. Conc. Res. 41 (1989) 51–61.
[29] S. Kelham, A water absorption test for concrete, Mag. Conc. Res. 40 (1988) 106–110.
[30] S.F. Wong, T.H. Wee, S. Swaddiwudhipong, S.L. Lee, Study of water movement in concrete, Mag. Conc. Res. 53 (2001) 205–220.
[31] N. Baghdadi, F. Toutlemonde, J.-F. Seignol, Modélisation de l'effet des contraintes sur l'anisotropie de l'expansion dans les bétons atteints de réactions de gonflement interne, XVèmes Rencontres de l'AUGC, Bordeaux, France, 2007.
[32] J.-M. Torrenti, L. Granger, M. Diruy, P. Genin, Modeling concrete shrinkage under variable ambient conditions, ACI Mater J. 96 (1999) 35–39.
[33] N. Baghdadi, Modélisation du couplage chimico-mécanique d'un béton atteint d'une réaction sulfatique interne, PhD Thesis, Ecole Nationale des Ponts et Chaussées, Marne la Vallée, France, 2008.
[34] N. Baghdadi, J.-F. Seignol, F. Toutlemonde, Modélisation du couplage chimico-mécanique pour calculer une structure en béton atteinte de réaction sulfatique interne, 18ème Congrès Français de Mécanique, Grenoble, France, 2007.